- Effect of deuteration degree of amphetamine on isotope effect in HPLC was studied
- Effect of structure of analyte, mobile phase and chiral selector on isotope effect in HPLC was studied
- Possible mechanisms of separation of isotopologues and enantiomers were studied.

Separation of isotopologues of amphetamine with various degree of deuteration on achiral and polysaccharide-based chiral columns in high-performance liquid chromatography

Giorgia Sprega[1], Giorgi Kobidze[1], Alfredo Fabrizio Lo Faro[1]*, Barbara Sechi[2], Paola Peluso[2], Tivadar Farkas[3], Francesco Paolo Busardò[1], Bezhan Chankvetadze[3]*

[1]Department of Excellence-Biomedical Sciences and Public Health, Università Politecnica delle Marche, 60121 Ancona, Italy

[2]Istituto di Chimica Biomolecolare ICB-CNR, Sede secondaria di Sassari, Traversa La Crucca 3, Regione Baldinca, Li Punti, 07100 Sassari, Italy

[3]Institute of Physical and Analytical Chemistry, School of Exact and Natural Sciences, Tbilisi State University, 0179 Tbilisi, Georgia

Corresponding authors: Alfredo Fabrizio Lo Faro, email: fabriziolofaro09@gmail.com

Bezhan Chankvetadze, e-mail: jpba_bezhan@yahoo.com

Abstract

Hydrogen/deuterium (H/D) isotope effects are not unusual in chromatography and such phenomena have been observed in both gas- and liquid-phase separations. Despite the numerous reports on this topic, the understanding of mechanisms and the underlying noncovalent interactions at play remains rather challenging. In our recent study, we reported baseline separation of isotopologoues of some amphetamine (AMP) derivatives on achiral and polysaccharide-based chiral columns, as well as some correlations between the degree of separation of enantiomers and isotopologues on (the same) polysaccharide-based chiral column(s). Following our previous findings on isotope effects in high-performance liquid chromatography, we report herein a comparative study on the isotope effects observed with AMP and methamphetamine (MET). The impact of some pivotal factors such as the number of deuterium atoms part of AMP isotopologues, the structure of its isotopomers, the chemical structure of the achiral and chiral stationary phases used in this study, and the use of methanol- vs acetonitrile-containing mobile phases on the isotope effects was examined and discussed. Quantitative correlations between the observed isotope effects and the enantioselectivity of the chiral columns used are also shortly discussed. Furthermore, considering the chromatographic results as benchmark experimental data, we attempted to elucidate the molecular bases of the observed phenomena using quantum mechanics calculations.

Keywords: Effect of deuterium atoms / Isotope effect in HPLC / Polysaccharide-based chiral columns / Separation of enantioisotopologues

1. Introduction

Isotopically labelled compounds have attracted increasing interest in the pharmaceutical industry in the last decade [1-5]. In particular, more and more attention is paid to the isotope kinetic effect [6] in biological (living) systems and among them in humans, in the sense that undeuterated and deuterated biologically active compounds may have different pharmacokinetic, toxicokinetic, and most likely even pharmacodynamic properties. Such differences led to the approval of some deuterated chemical species as drugs for clinical use by regulatory bodies since 2017 [1-5]. Contrary to this, in bioanalysis it is believed that isotope effects do not play any significant role or don't even exist and therefore, isotopically labelled (primarily deuterated) analogues of target analytes are considered to be optimal internal standards in bioanalysis with mass-spectrometric (MS) detection [7,8]. Thus, remarks like this "*Ideally, a stable-isotope labeled internal standard is preferred whenever possible, as it has exactly the same structure as the analyte and co-elutes with it.*" [7] are quite common in the scientific literature. This belief translates into the following practical consequences: nonlabelled and isotopically labelled compounds extract from biological matrixes most likely to the same degree, have the same solubility in specific solvents, have the same pK values, the same retention in given chromatographic systems (column + mobile phase), etc. Such assumptions mean that isotopologues cannot be chromatographically separated. However, when mass-spectrometric detection is used, isotopologues can be differentiated and selectively detected and quantified based on their different molecular mass. The coelution of the undeuterated and deuterated forms of a given analyte is generally considered advantageous in LCMS analysis with the expectation that both species experience the same degree of ion enhancement or suppression in the ion source [7,8].

Over the past decades, significant isotope effects have been observed in gas chromatography [9-16], in various modes of liquid chromatography, such as ion-exchange [17], normal phase [18], reversed-phase [19-23] and chiral [24-26] chromatography, as well as

70 in electrokinetic chromatography [27,28]. Two types of isotope effects are known in
71 chromatography, i.e. the “normal” and the “inverse” isotope effect. The former refers to cases
72 when the heavier deuterated isotopologues retain longer compared to lighter protiated
73 counterparts, whereas the “inverse” isotope effect is observed when lighter isotopologues
74 retain longer compared to heavier counterparts. The presence of either isotope effect is
75 contrary to the expectations of most analysts, and a challenge in bioanalysis [23]. On the other
76 hand, the isotope dilution method is based on the presence of such an isotope effect and
77 enables using isotopically labelled internal standards without the use of MS detection [13,19].
78 In addition, Rudaz and co-authors have demonstrated that for quantification with a mass
79 spectrometric detector it may be advantageous that nonlabelled and isotopically labelled
80 internal standard elute with different retention factors. This means that the presence of the
81 isotope effect favors adequate quantification [24].

82 In a recent study, we observed that the isotope effect was tunable and dependent on
83 mobile phase composition in high-performance liquid chromatography (HPLC) for several
84 AMP derivatives [26]. Under the studied conditions, a stronger isotope effect was observed in
85 acetonitrile-containing mobile phases compared to methanol-containing ones with both chiral
86 and achiral columns and both “normal” and “inverse” isotope effects were observed. Whereas
87 the former was favored in polar organic solvents, increasing the content of the aqueous
88 component in the reversed-phase mobile phase favored an “inverse” isotope effect.
89 Preliminary quantum mechanics calculations supported the hypothesis that polar, hydrogen
90 bonding-type noncovalent interactions are involved in the “normal” isotope effect, while
91 apolar, hydrophobic-type interactions underlie the “inverse” isotope effect.

92 Following our previous study, we describe herein a study on the isotope effects
93 observed on AMP and MET isotopologues. In this frame, the impact of the number of
94 deuterium atoms part of AMP isotopologues, the structure of isotopomers, the chemical

structure of the achiral and chiral stationary phases used in this study, and the use of methanol- vs. acetonitrile-containing mobile phases on the isotope effects are reported and examined. Quantitative correlations between the isotope effect and the enantioselectivity of the chiral columns used are also shortly discussed. With the aim of elucidating the molecular bases of the observed phenomena, quantum mechanics calculations were performed focusing on the vibrational degree of freedom calculated for low-energy conformers of both AMP and MET isotopologues as well as related zero-point vibrational energies as descriptors useful to differentiate computationally isotopologues and isotopomers.

2. Experimental

2.1. Materials

The chiral test compounds amphetamine (AMP), amphetamine-$d_{5(ring)}$ (AMP-$d_{5(ring)}$), methamphetamine (MET) and methamphetamine-d_5 (MET-d_5) were commercially available from Cerilliant (Round Rock, TX, USA). S-(+)-amphetamine (S-(+)-AMP), amphetamine-$d_{5(side\ chain)}$ (AMP-$d_{5(side\ chain)}$), amphetamine-d_6 (AMP-d_6), amphetamine-d_8 (AMP-d_8) and amphetamine-d_{11} (AMP-d_{11}) were purchased from Sigma Aldrich (Milan, Italy). Standards were stored at -20° C until used in analysis. The structures of the studied analytes are shown in Fig 1. HPLC-grade methanol, acetonitrile and water were supplied by Carlo Erba (Cornaredo, Italy). Ammonium hydroxide (25% w/w aqueous solution) and ammonium bicarbonate (98.5% purity) were purchased from Honeywell Fluka™ (Morristown, NJ, USA). The chiral columns Lux-AMP, Lux i-Amylose-3 (with amylose tris(3-chloro-5-methylphenylcarbamate) as a chiral selector) and Lux Cellulose-3 (based on cellulose tris(4-methylbenzoate) as a chiral selector), as well as all achiral columns such as Kinetex 2.6 µm Phenyl-Hexyl, Kinetex 2.6 µm Biphenyl and Luna Omega 1.6 µm Polar C18 were provided by Phenomenex Inc. (Torrance, CA, USA). Lux Cellulose-3 and Lux i-Amylose-3 both

120 packed with the particles of 5 μm nominal size and the Lux AMP column packed with the
121 particles of 3 μm nominal size all were of 250 x 4.6 mm dimensions. All 3 achiral columns
122 were of 100 x 2.1 mm dimensions.

123

124 *2.2. High-performance liquid chromatography tandem mass spectrometry (HPLC-MS/MS)*
125 *analysis*

126 A HPLC 1290 Infinity II (Agilent Technologies Italia S.p.a., Milan, Italy) instrument
127 coupled with a mass spectrometer (6470A Triple Quadrupole LC-MS) equipped with an
128 electrospray ionization source (ESI) operating in both positive and negative mode was used.
129 Data were acquired with MassHunter® Workstation Qualitative Analysis 10.0 Software
130 (Agilent). Analysis of all compounds were performed on three chiral and three achiral
131 columns (for their characteristics see above). Isocratic elution mode was adopted in all
132 experiments. In case of Lux AMP column which is unique columns with pH stability in the
133 range 1.0-11.5, methanol with 0.1% ammonium hydroxide was initially used as mobile phase,
134 while later the mobile phase was composed of methanol and 5 mM ammonium bicarbonate
135 (pH=11.0, adjusted with ammonium hydroxide) in water in the ratio 95/5 (v/v). Also, the
136 content of methanol was decreased in 5% steps down to 20/80 (v/v) ratio of methanol to 5
137 mM ammonium bicarbonate in water. The same procedure was used with acetonitrile as
138 mobile phase organic component. In case of the other five columns (two chiral and three
139 achiral) the same approach was used, but without adjusting the pH of 5 mM ammonium
140 bicarbonate solution which was used at its native pH=7.7. For the chiral columns (of 4.6 mm
141 i.d.) 1 ml/min mobile phase flow rate was used.

142 In case of the Kinetex 2.6 μm Phenyl-Hexyl column, 0.5 ml/min flow rate was used
143 with methanol, while 0.4 ml/min with acetonitrile containing mobile phases. The Kinetex 2.6

144 µm Biphenyl column was operated at 0.4 ml/min mobile phase flow rate. The Luna Omega
145 1.6 µm Polar C18 column was operated at 0.4 ml/min flow rate with acetonitrile in
146 combination with 5 mM ammonium bicarbonate in water as mobile phase. The same column
147 operated with methanol in combination with 5 mM ammonium bicarbonate in water
148 experienced excessive backpressure. For this reason, all experiments using such mobile phase
149 were executed at 0.2 ml/min mobile phase flow rate. Autosampler and column oven
150 temperatures were set to 10° C and 25° C, respectively. The mass spectrometer was operated
151 in scheduled multiple reaction monitoring (MRM) mode for the analyte and internal standard,
152 with two transitions each (Table 1). Scan speed (dwell time) was set to 0.023 sec. ESI
153 conditions were optimized as follows: capillary voltage 3500 V, source temperature 300° C,
154 cone gas flow rate 10 L/min, desolvation gas flow rate 12 L/min.

155

156 *2.3. Computations*

157 The 3D structures of AMP and MET were prepared by using the build function, and
158 model kits and tools provided by Spartan' 10 Version 1.1.0 (Wavefunction Inc., Irvine, CA,
159 USA) [29] for building and editing organic molecules. On this basis, the structures of these
160 molecules were generated, and their refinement was performed by a MMFF procedure. Then,
161 each structure was submitted to a conformational search through a systematic algorithm by
162 using the MMFF force field, spanning all shapes accessible to the molecule without regard to
163 energy. After elimination of three high-energy conformers (Boltzmann Distribution % ≤ 0.1), a
164 set of 15 energetically accessible conformers was selected in both cases. For each conformer,
165 geometry optimization was performed in gas phase at density functional theory (DFT) level
166 with the B3LYP functional and the 6-31G(d) basis set. For each compound, two low-energy
167 conformers were selected and their geometry was optimized with Gaussian 16W (Wallingford,
168 CT, USA) [30] using tight convergence criteria, D3 version of Grimme's dispersion with the

original D3 damping function [31], and the solvation model based on density (SMD) (acetonitrile, methanol, and water) variation of IEFPCM (integral equation formalism for polarizable continuum model) of Truhlar and co-workers [32]. Computation of electrostatic potential (V) values mapped on electron density isosurfaces (V_S) was performed. Search for the exact location of $V_{S,max}$ was extracted from the .wfn files through the Multiwfn code [33] and through its module enabling quantitative analyses of molecular surfaces (isovalue 0.001 au) [34]. The .wfn files for AMP and MET, and the vibrational wavenumbers for AMP and MET isotopologues were calculated by using Gaussian 16W (Wallingford, CT, USA) [30] [DFT/B3LYP/6-31G(d)]. The energy of the optimized structures of the complexes of MET with benzene, 1,3-dimethylbenzene, and 1-chloro-3-methylbenzene were calculated at DFT level with the B3LYP functional, the 6-31+G(d,p) as basis set, and the D3 version of Grimme's dispersion with Becke-Johnson damping [35].

3. Results and Discussion

Separation and enantioseparation of AMP and MET isotopologues, i.e. AMP, AMP-$d_{5(side\ chain)}$, AMP-$d_{5(ring)}$, AMP-d_6, AMP-d_8, AMP-d_{11}, MET and MET-d_5, were systematically explored by using the Kinetex Biphenyl (Supporting Information, Tables S1-S3 and Figs. S1-S3) and Phenyl-Hexyl achiral columns, and Lux AMP (Tables S4-S6, Figs. S4 and S5), Lux Cellulose-3 and Lux i-Amylose-3 (Tables S7-S9, Figs. S6 and S7), as chiral columns, at different contents of water in aqueous MeOH and ACN mixtures used as mobile phases.

3.1. Effect of achiral and chiral column stationary phase on isotope effect

The isotope effect observed with the Biphenyl column in methanol was weak. It was positive (i.e. the heavier isotopologues retained longer compared to the lighter ones) in

methanol containing 0.1% (v/v) ammonium hydroxide and methanol containing a low amount of aqueous phase and turned negative (i.e. lighter isotopologues retained longer compared to the heavier ones) with increasing amount of aqueous component in the mobile phase. The same trend was observed for MET as for AMP and its isotopologues (Supporting Information, Table S3 and Fig. S3). The effect observed with the Phenyl-Hexyl column was very similar to the one observed on the Biphenyl column.

On the chiral Lux AMP column AMP and its isotopologues were retained very long (for over 40 minutes) and peaks were severely distorted in methanol without any additive. In this mobile phase, the positive isotope effect was observed. However, in contrast to the abovementioned achiral columns, there was no positive isotope effect observed, not even in methanol containing 0.1% ammonium hydroxide. In fact, there was a very weak, almost negligible, negative isotope effect in methanol with 0.1% ammonium hydroxide [ΔRT (AMP-AMP-$d_{5(\text{side chain})}$ = 0.001 min] that increased with increasing content of the aqueous component in the mobile phase (Figs. 2a-c). The separation of isotopologues and enantiomers correlated very well with each other (Figs. 2a-c). Specifically, with increasing aqueous content in the mobile phase both, the extent of the negative isotope effect, as well as the separation selectivity of AMP-enantiomers increased significantly (Fig. 2). The same observation was made for MET under the same experimental conditions (Fig. 3).

On the chiral i-Amylose-3 column there was no measurable isotope effect in methanol containing 0.1% ammonium hydroxide but with addition of 5% (v/v) aqueous buffer a significant positive isotope effect appeared (Fig. 4) which is different from the observation made with the Lux AMP column. With increasing content of the aqueous mobile phase, the positive isotope effect reversed to negative and at a high content of aqueous component also enantioseparation appeared (This is another example of a correlation between the negative isotope effect and enantioseparation) (Fig. 4). With MET, positive isotope effect was observed

on i-Amylose-3 while no enantioseparation in any methanol-containing mobile phases (Table S9).

A rather weak (mostly negative) isotope effect was observed on the Lux Cellulose-3 column for both AMPs and MET in methanol-containing mobile phases, while a weak positive isotope effect was observed in ACN-containing mobile phases (Data not shown). The enantiomers of AMP and MET were not separated on this column under the conditions studied.

From these experimental results some remarks emerged:

1. The negative isotopic effect was favoured by mobile phases containing higher percentages of water. In all cases, retention times increased significantly as the water content in the mobile phase increased (typical reversed-phase behaviour although at lower content of water (up to 20% mostly) HILIC-like retention was observed).
2. With the two amylose-based columns, i.e. Lux AMP and i-Amylose-3, the type and extent of the isotope effect as well as of enantioseparation could be affected by the stereoelectronic features of the pendant groups.

3.2. Isotope effect in relation to methanol vs. acetonitrile and amphetamines vs. methamphetamines

As mentioned in subsection 3.1 only a weak isotope effect was observed for both, AMP and MET in methanol on the Biphenyl column while a significant difference was observed on the same column in ACN between these compounds. In particular, only a marginal isotope effect was observed for AMPs in ACN containing 0.1% ammonium hydroxide ($\Delta RT = 0.001$ min), while a quite strong positive isotope effect was observed for

MET in the same separation system (Fig. 5). The observation on the Phenyl-Hexyl column in ACN vs. methanol was very similar to that on the Biphenyl column (Data not shown).

On the chiral Lux AMP column, good separation of AMP enantiomers and only very weak (almost undetectable) positive isotope effect was observed in ACN containing 0.1 % ammonium hydroxide. With the addition of an initial amount of the aqueous component (see experimental section) HILIC behavior was observed as reported in our multiple studies leading to a reduction in retention factors and enantioseparation [26,36-39]. Already at 5% (v/v) content of the aqueous component in the mobile phase the isotope effect turned negative and gradually increased in correlation with enantioseparation (Table S5 and Figure S5). MET showed a significant difference from AMP with positive isotope effect observed in ACN and lower content of aqueous buffer. This positive isotope effect disappeared and then flipped to negative isotope effect with increasing content of the aqueous component in the mobile phase without achieving separation of enantiomers (Supporting information, Table S6).

On the Lux i-Amylose-3 column there was no measurable isotope effect for AMP, and its enantiomers were not separated in ACN modified with 0.1% (v/v) ammonium hydroxide, while for MET under the same experimental conditions there was a quite strong positive isotope effect, as well as MET enantiomers were significantly separated from each other (Fig. 6).

The experimental results obtained for the separation and enantioseparation performed with acetonitrile-containing mobile phases showed that under these conditions the positive effect tended to be favored, while the negative effect could be observed with mobile phases containing higher percentages of water. In this regard, it is worth mentioning that acetonitrile favors and disfavors hydrogen-bonding (HB) and hydrophobic interactions between the chiral selector and analyte species, respectively, in contrast to methanol which manifests the opposite effects.

3.3. Correlations between the extent of the isotope effect and the number and location of deuterium atoms in the molecule

There are a few reports in the literature on the effect of the number of deuterium atoms part of the isotopologue on the extent of the isotope effect [20,25]. This aspect was systematically examined in the present study. As shown in Fig. 7, a certain correlation was observed, and in some cases the isotope effect increased with increasing number of deuterium atoms in the molecule. As already mentioned in earlier studies [20,25] the isotope effect does not increase linearly with the number of deuterium atoms part of the molecule and the so-called specific deuterium effect (incremental isotope effect per added deuterium atom to the molecule) decreases with increasing the degree of deuteration of a molecule. Moreover, it is obvious that not just the number of deuterium atoms but also their location in the structure of molecule plays a certain role in the observed effect. On one hand, this observation suggests that the separation of isotopomers is possible and correlates with the successful separation of racemates based on isotopic chirality reported by Tanaka and co-workers [40]. On the other hand, this observation suggests that not only mass-dependent forces are responsible for the separation of isotopologues.

In the present study, differences between isotopomers were also examined (Fig. 7 and Supporting Information, Fig. S8). In this regard, it is evident that a minor difference observed in the retention of isotopomers is (as expected) insufficient to observe their separation under the used experimental conditions. However, interesting trends could be observed by examining the variations in the retention times of the various isotopologues (or isotopomers) as the chromatographic conditions changed:

1. Slightly stronger isotope effect was observed for the isotopologue/isotopomer containing deuterium atoms in the side chain compared to that on the aromatic ring.

2. In several cases, the retention of AMP-d_8, not containing deuterium atoms at C_α and C_β with respect to the NH_2 group, was lower than expected, deviating from the linear-like trend exhibited by the other isotopologues of the series.

3. On the Lux AMP column, the retention of AMP-$d_{5(ring)}$ was slightly lower compared to AMP-d_6 and AMP-d_{11} with ACN containing 0.1 % ammonium hydroxide, whereas it was higher with a mobile phase containing high percentages of water (Supporting Information, Fig. S9).

3.5. Possible recognition mechanism underlying isotope effects

In spite of the importance of isotope effects in analytical and bioanalytical separations, studying the mechanisms and noncovalent interactions underlying these effects by computational analysis remains rather challenging. The main question arises from the fact that, under the Born-Oppenheimer approximation, the potential energy surfaces of different isotopes are the same. Consequently, the difference in the thermodynamic stability between two isotopomers (or isotopologues) can arise exclusively from the vibrational frequency of C–H and C–D bonds [41]. Indeed, the C–D bond presents smaller vibrational frequency, shorter bond length, and lower polarizability compared to the C–H bond [42]. Given these subtle differences, a very small or non-detectable difference between isotopologues was observed so far [43], and various methodological approaches often provided opposite results. For instance, whereas studies on the encapsulation of protic and deuterated guest molecules in molecular capsules led to the conclusion that the C–D···π interaction is stronger than the C–H···π interaction [44], others based on chromatographic analysis led to the opposite conclusion. In this field, Tanaka and co-authors studied the hydrogen/deuterium isotope effects on hydrophobic binding in the reversed-phase chromatographic separation of protiated and deuterated isotopologues, observing that protiated compounds bind to nonpolar moieties attached to silica more strongly

than the deuterated ones [21]. Later, by the comparison of the free energies of isotopologues derived in RPLC, Kubo and co-authors hypothesized that the C–H···π interaction was slightly stronger than C–D···π interaction providing an inverse isotope effect in the separation of aromatic hydrocarbons [22]. Therefore, the contribution of dispersion forces to H/D isotope effects was not conclusively confirmed so far.

On this basis, we studied molecular and electronic properties of AMP and MET conformers optimized at DFT level of theory (Supporting Information, Table S10). The calculations were performed by using the implicit SMD as solvation model in three different solvents, i.e. acetonitrile, methanol, and water, in agreement with the experimental mobile phases. In all cases, two types of lowest-energy conformers were found. The first conformer type (conformer **a**) featured an intramolecular C–H···π interaction (2.817 Å $\leq d_{CH\cdots\pi} \leq$ 2.835 Å) underlying the structure, with the amine hydrogen(s) available as HB donor(s). In the other conformer type (conformer **b**), the amine hydrogen was found involved in the intramolecular NH···π interaction (2.551 Å $\leq d_{NH\cdots\pi} \leq$ 2.697Å), thus it was not available for intermolecular HBs due to stereoelectronic reasons. In particular, conformer **b** of MET exposes an extended hydrophobic surface on the opposite side from the NH group. The calculated properties showed that MET presents a higher contribution of dispersion to the total energy and higher polarizability compared to AMP. To the contrary, this latter shows, in general, lower electron charge density, and more positive electrostatic potential maxima on the amine hydrogens that, consequently, exhibited higher ability as HB donors. Furthermore, the amine nitrogen of AMP featured a more negative value of electrostatic potential, thus higher electron charge density, compared to the amine nitrogen of MET. On this basis, the higher retention of MET observed in all cases compared to AMP could be ascribed to dispersion-type forces rather than to HB-type forces. On this basis, to evaluate the possible contribution of dispersion forces in the studied analytical (enantio)separations, we calculated the energy of the complexes between

conformer **b** of MET and benzene, 1,3-dimethylbenzene, and 1-chloro-3-methylbenzene to explore the impact of the electronic properties of the substituents on benzene (methyl and/or chlorine) on the contribution of the dispersion energy to the overall binding energy. As shown in Fig. 8, in all cases a CH···π interaction between one methylene hydrogen of MET and the aromatic counterpart was observed, as well as a calculated contribution of the dispersion to the total energy increasing following the order benzene (-0.0750 au) < 1-chloro-3-methylbenzene (-0.0881 au) < 1,3-dimethylbenzene (-0.0912 au). In this regard, it is worth mentioning that noncovalent interactions like C–H···π present a high character as dispersive forces [45].

Based on these computed results and on the structural features of AMP and MET, our mechanistic hypotheses were the following:

1. The medium determines the equilibrium between the conformers of the analyte in solution, whereas the structure of the (chiral) selector determines how the system of the two conformers at the equilibrium interacts with (chiral) selector. Indeed, the relative stability of conformers **a** and **b** depended on the medium. On the other hand, the energy differences were very low [$\Delta E = E_{\text{conformer b}} - E_{\text{conformer a}}$: 0.19 kcal/mol (ACN), 0.15 kcal/mol (MeOH), and 0.06 kcal/mol (water) for AMP and 0.53 (ACN and MeOH), and 0.51 (water) for MET]. Thus, it was expected that the two conformers could interconvert rather easily.

2. Separation and enantioseparation outcomes depend on a subtle balance between HB and dispersive forces.

3. Depending on the location of the deuterium atoms, deuteration favored HB and disfavored dispersive forces. Indeed, as reported before [26], deuterium is more electronegative compared to protium when bound to a Csp^3. Thus, deuterated groups close to the N-H moiety in the analyte structure can cause its stronger (increased) deshielding (meaning higher hydrogen-bonding donor capacity) compared to the N-H group in the nondeuterated analyte.

On the other hand, the frequency of vibration is inversely proportional to the mass of the atoms, so heavier atoms vibrate at lower wavenumbers. The C–H bond has a higher oscillation frequency than the C–D bond (the wavenumbers are 3300 vs. 2334 cm^{-1}, respectively). Thus, it may induce stronger dispersion attraction. This could result in higher retention for the undeuterated compound compared to its deuterated analogue due to the difference in dispersive analyte-adsorbent interactions.

Given these hypotheses, we calculated (Supporting information, Tables S11-S18) and compared (Supporting information, Tables S19-S24) in detail the vibration wavenumbers of the two conformers of AMP and MEP in the three solvents. Indeed, the amount of energy required to stretch a bond depends on the strength of the bond and the masses of the bound atoms, and the stronger is the bond, the greater is the energy required to stretch it. Thus, by comparing the stretching wavenumbers of N-H groups part of different isotopologues, we could evaluate how the strength of the HB involving the N-H groups changes. In terms of dispersion forces, we considered the zero-point vibrational energy (ZPVE) as descriptor to compare the dispersion capability of the different isotopologues. Indeed, the ZPVE results from the vibrational motion of molecular systems at 0 K, and it is calculated for a harmonic oscillator model as a sum of contributions for all vibrational degrees of freedom of the system.

$$\mathrm{ZPVE} = \Sigma_i \, 0.5 h c \tilde{\nu}_i \qquad (1)$$

where h is the Plank constant, c the light speed, $\tilde{\nu}$ the vibrational wavenumber, and i refers to the vibrational degrees of freedom.

Interesting correlations between the calculated vibrational wavenumbers and the experimental retention times were observed:

1. In all cases, lower $\tilde{\nu}_{N\text{-}H}$ were calculated for the isotopologues containing deuterium atoms at Cα and Cβ with respect to the NH_2 group, i.e. AMP-$d_{5(\text{side chain})}$,

390 AMP-d_6, an AMP-d_{11} compared to AMP, AMP-d_8, and AMP-$d_{5(ring)}$. Thus, for the
391 first series stronger HB donor ability could be expected.
392 2. The ZPVE increased as the deuteration degree and solvent polarity (ACN
393 < MeOH < water) increased.
394 3. For both conformers of AMP, higher ZPVE was calculated for AMP-
395 $d_{5(ring)}$ compared to AMP-$d_{5(side\ chain)}$.

396 These results confirmed a close relationship between the retention times observed in the
397 chromatographic experiments and the descriptors used to quantify the contribution of HB and
398 dispersive forces to retention and in enantioseparation mechanisms, and in almost all cases, the
399 lines describing the dependence of retention on the deuteration degree correlated satisfactorily
400 with the lines describing the dependence of the vibrational wavenumbers on the deuteration
401 degree. In Figs. 9 and 10, some representative correlations are reported for the separation of
402 AMP isotopologues with the Biphenyl column and MeOH/water 90:10, 20:80, and 70:30 as
403 mobile phases. At lower concentration of water (10%) (Fig. 9A), the HB dominates the retention
404 mechanism and retention time of AMP_conformer **a** (SMD, MeOH) increases or decreases as
405 the $\tilde{\nu}_{N\text{-}H}$ decreases (HB ability increases) or increases (HB ability decreases). In the opposite
406 situation, at higher concentration of water (80%) (Fig. 9B), the retention time clearly depended
407 on the ZPVE value, thus in this case the contribution of dispersive forces to the mechanism was
408 dominant. At intermediate percentages of water (30%) (Fig. 10), retention time depended on
409 the balance between HB and dispersive forces (r^2 = 0.9525). In particular, the decrease in
410 retention time moving from AMP-d_6 to AMP-d_8 could be explained by the corresponding
411 increase in the $\tilde{\nu}_{N\text{-}H}$ (decrease in HB donor ability).

412 This model could explain other experimental behaviors:

413 1. The explanation of the differences observed between AMP and MET on both
414 Biphenyl and Lux AMP column with ACN, i.e. almost no isotope effect for AMP and a stronger

positive isotope effect for MET, could be found in the difference in the $\tilde{\nu}_{N\text{-}H}$ of the protiated and the $d_{5(side\ chain)}$ isotopologues calculated in the two cases, higher for MET [$\Delta\tilde{\nu}_{N\text{-}H} = \tilde{\nu}_{N\text{-}H}$ (MET) - $\tilde{\nu}_{N\text{-}H}$ (MET-$d_{5(side\ chain)}$) = 0.19 cm^{-1}] compared to AMP [$\Delta\nu_{N\text{-}H} = \tilde{\nu}_{N\text{-}H}$ (AMP) - $\tilde{\nu}_{N\text{-}H}$ (AMP-$d_{5(side\ chain)}$), 0.01 $cm^{-1} \leq \Delta\tilde{\nu}_{N\text{-}H} \leq$ 0.09 cm^{-1}].

2. For the (enantio)separation of AMP-$d_{5(side\ chain)}$, AMP-d_6, AMP-d_{11}, and AMP-$d5_{(ring)}$ series with the Lux AMP column in ACN-containing mixture, the retention time order ($d_{5(ring)} < d_{11}$, d_6 , $d_{5(side\ chain)}$) in pure ACN correlated well with the change in $\tilde{\nu}_{N\text{-}H}$ ($d_{5(ring)} > d_{11}$, d_6 , $d_{5(side\ chain)}$), whereas retention time changed (Fig. S9) as the ZPVE values at the highest percentages of water (80%) [RT(1) (min), ZPVE AMP_a (SMD, water) (H/particle): $d_{5(ring)}$ (26.85, 0.186800) > $d_{5(side\ chain)}$ (26.66, 0.186654) > d_6 (26.50, 0.183278) > d_{11} (25.27, 0.166848)].

4. Conclusions

A strong isotope effect was observed for partially deuterated AMP derivatives under some experimental conditions enabling their baseline separation on achiral and polysaccharide-based chiral columns in HPLC. The nature (positive or negative) of the isotope effect and its extent strongly depends on the nature of selector, medium and structure of the studied compounds. On chiral columns some correlations were observed between the strength of the isotope effect and selectivity of enantioseparation. The isotope effect increased with increasing number of deuterium atoms in the molecule. Some differences in the retention of isotopomers were observed but this was not sufficient for their separation. Analysis of the vibrational wavenumbers and related ZPVE calculated for both AMP and MET isotopologues by quantum mechanics allowed to disclose some essential factors contributing to retention and enantiorecognition, profiling a model based on the interplay between HB- and dispersive-type interactions. The number and location of the deuterium atoms in the AMP and the MET impact the strength of these interactions. Increasing deuteration degree, in particular at

positions close to the amino group, was found to favor hydrogen bonding-type forces, whereas it was detrimental to dispersive forces.

This study reporting on concomitant significant differences observed in the isotope effect and enantioseparation based on the structure of the chiral selector, mobile phase and the structure of analytes may provide important material for better understanding of enantioselective recognition mechanisms.

CRediT authorship contribution statement

Giorgia Sprega, Giorgi Kobidze, Barbara Sechi: Formal analysis, Investigation**. Alfredo Fabrizio Lo Faro:** Formal analysis, Investigation, Supervision. **Paola Peluso:** Conceptualization, Methodology, Formal analysis, Investigation**,** Writing. **Tivadar Farkas:** Writing – review & editing, Resources. **Francesco Paolo Busardò:** Conceptualization, Methodology, Formal analysis, Investigation, Supervision, Resources. **Bezhan Chankvetadze:** Conceptualization, Methodology, Formal analysis, Investigation, Supervision, Validation, Writing – original draft, Writing – review & editing.

Declaration of Competing Interest

The authors declare that they have no known competing financial interests or personal relationships that could have appeared to influence the work reported in this paper.

Acknowledgements

Bezhan Chankvetadze thanks Department of Excellence-Biomedical Sciences and Public Health, Università Politecnica delle Marche for providing financial support for his stay in

463 Ancona as Visiting Professor. He also thanks Shota Rustaveli National Science Foundation of
464 Georgia for a partial support of this study through the grant N◦ FR-22–971 for fundamental
465 research.

466

5. References

[1] J. Atzrodt, V. Derdau, W.J. Kerr, M. Reid, Deuterium-and tritium-labelled compounds: applications in the life sciences, Angew. Chem. Int. Ed. Engl. 57 (2018) 1758-1784. doi:10.1002/anie.201704146.

[2] C. Schmidt, First deuterated drug approved, Nat. Biotechnol. 35 (2017) 493-494. doi:10.1038/nbt0617-493.

[3] S.J. Keam, S. Duggan, Donafenib: first approval. Drugs 81 (2021) 1915-1920. doi:10.1007/s40265-021-01603-0.

[4] S.T. Wrobleski, R. Moslin, S. Lin, Y. Zhang, S. Spergel, J. Kempson, J.S. Tokarski, J. Strnad, A. Zupa-Fernandez, L. Cheng, D. Shuster, K. Gillooly, X. Yang, E. Heimrich, K.W. McIntyre, C. Chaudhry, J. Khan, M. Ruzanov, J. Tredup, D. Mulligan, D. Xie, H. Sun, C. Huang, C. D'Arienzo, N. Aranibar, M. Chiney, A. Chimalakonda, W.J. Pitts, L. Lombardo, P.H. Carter, J.R. Burke, D.S. Weinstein, Highly selective inhibition of tyrosine kinase 2 (TYK2) for the treatment of autoimmune diseases: discovery of the allosteric inhibitor BMS-986165, J. Med. Chem. 62 (2019) 8973-8995. doi:10.1021/acs.jmedchem.9b00444.

[5] R.M.C. Di Martino, B.D. Maxwell, T. Pirali, Deuterium in drug discovery: progress, opportunities and challenges, Nat. Rev. Drug Discov. 22 (2023) 562-584. doi:10.1038/s41573-023-00703-8.

[8] J. Bigeleisen, M.G. Mayer, Calculation of equilibrium constants for isotopic exchange reactions, Int. J. Chem. Phys. 261 (1947) 261-267. https://doi.org/10.1063/1.1746492.

[6] Y. Fu, D. Barkley, W. Li, F. Picard, J. Flarakos, Evaluation, identification and impact assessment of abnormal internal standard response variability in regulated LC−MS bioanalysis, Bioanalysis 12 (2020) 545-559. doi:10.4155/bio-2020-0058.

[7] L. Heinle, K. Sulaiman, A. Olson, K. Ruterbories, A homologous series of internal standards for near universal application in the discovery LC-MS/MS bioanalytical laboratory, J. Pharm. Biomed. Anal. 190 (2020) 113578. doi:10.1016/j.jpba.2020.113578.

[9] K.E. Wilzbach, P. Riesz, Isotope Effects in Gas-Liquid Chromatography, Science 126 (1957) 748-749. doi:10.1126/science.126.3277.748.

[10] S. Ohkoshi, Y. Fujita, T. Kwan, Gas chromatographic separation of hydrogen isotopes D2 and HD, Bull. Chem. Soc. Jpn. 31 (1958) 770-771. https://doi.org/10.1246/bcsj.31.770.

[11] F. Bruner, G. Cartoni, A. Liberti, Gas chromatography of isotopic molecules on open tubular columns, Anal. Chem. 38 (1966) 298-303. https://doi.org/10.1021/ac60234a035.

[12] B. Shi, B.H. Davis, Gas chromatographic separation of pairs of isotopic molecules. J. Chromatogr. A 654 (1993) 319-325. https://doi.org/10.1016/0021-9673(93)83377-5.

[13] H.G. Schmarr, M. Wacker, M. Mathes, Isotopic separation of acetaldehyde and methanol from their deuterated isotopologues on a porous layer open tubular column

allows quantification by stable isotope dilution without mass spectrometric detection, J. Chromatogr. A. 1481 (2017) 111-115. doi:10.1016/j.chroma.2016.12.023.

[14] N. Thakur, S. Aslani, D.W. Armstrong, Evaluation of gas chromatography for the separation of a broad range of isotopic compounds, Anal. Chim. Acta 1165 (2021) 338490. doi:10.1016/j.aca.2021.338490.

[15] S. Aslani, D.W. Armstrong, Effect of position of deuterium atoms on gas chromatographic isotope effects, Talanta 265 (2023) 124857. doi:10.1016/j.talanta.2023.124857.

[16] M.D. Chermá, G.H. Nilsson, A. Johansson, A.K. Jönsson, J. Ahlner, Use of Lisdexamfetamine or Amphetamine? Interpretation of Chiral Amphetamine Analyses, J. Anal. Toxicol. 46 (2022) 10-16. doi:10.1093/jat/bkaa170.

[17] H. Gottschling, E. Freese, A tritium isotope effect on ion exchange chromatography, Nature 196 (1962) 829-831. doi:10.1038/196829a0.

[18] S.S Iyer, K.P. Zhang, G.E. Kellogg, H.T. Karnes, Evaluation of deuterium isotope effects in normal-phase LC-MS-MS separations using a molecular modeling approach, J. Chromatogr. Sci. 42 (2004) 383-387. doi:10.1093/chromsci/42.7.383.

[19] J.J. Pratt, Isotope dilution analysis using chromatographic separation of isotopic forms of the compound to be measured, Ann. Clin. Biochem. 23 (1986) 251-276. doi:10.1177/000456328602300305.

[20] C.F. Masters, S.P. Markey, I.N. Mefford, M.W. Duncan, Separation of deuteriated isotopomers of dopamine by ion-pair reversed-phase high-performance liquid chromatography, Anal Chem. 60 (1988) 2131-2134. doi:10.1021/ac00170a029.

[21] M. Turowski, N. Yamakawa, J. Meller, K. Kimata, T. Ikegami, K. Hosoya, N. Tanaka, E.R. Thornton, Deuterium isotope effects on hydrophobic interactions: the importance of dispersion interactions in the hydrophobic phase, J. Am. Chem. Soc. 125 (2003) 13836-13849. doi:10.1021/ja036006g.

[22] E. Kanao, T. Kubo, T. Naito, T. Sano, M. Yan, N. Tanaka, K. Otsuka, Tunable Liquid Chromatographic Separation of H/D Isotopologues Enabled by Aromatic π Interactions, Anal. Chem. 92 (2020) 4065-4072. doi:10.1021/acs.analchem.9b05672

[23] S. Szarka, K. Prokai-Tatrai, L. Prokai, Application of screening experimental designs to assess chromatographic isotope effect upon isotope-coded derivatization for quantitative liquid chromatography-mass spectrometry, Anal. Chem. 86 (2014) 7033-7040. doi:10.1021/ac501309s

[24] S. Souverain, C. Eap, J.L. Veuthey, S. Rudaz, Automated LC-MS method for the fast stereoselective determination of methadone in plasma, Clin. Chem. Lab. Med. 41 (2003) 1615-1621. doi:10.1515/CCLM.2003.245.

[25] A. Valleix, S. Carrat, C. Caussignac, E. Léonce, A. Tchapla, Secondary isotope effects in liquid chromatography behaviour of 2H and 3H labelled solutes and solvents, J Chromatogr A 1116 (2006) 109-126. doi:10.1016/j.chroma.2006.03.078.

[26] G. Kobidze, G. Sprega, G. Daziani, A. Balloni, A.F. Lo Faro, T. Farkas, P. Peluso, G. Basile, F.P. Busardò, B. Chankvetadze, Separation of undeuterated and partially deuterated enantioisotopologues of some amphetamine derivatives on achiral and polysaccharide-based chiral columns in high-performance liquid chrom (atography, J. Chromatogr. A. 1718 (2024) 464709. doi:10.1016/j.chroma.2024.464709.

[27] M.M. Bushey, J.W. Jorgenson, Separation of Dansylated Methylamine and Dansylated Methyl-d3-amine by Micellar Electrokinetic Capillary Chromatography with Methanol-Modified Mobile Phase, Anal. Chem. 61 (1989) 491-493. doi:10.1021/ac00180a022.

[28] M.M. Bushey, J.W. Jorgenson, Effects of methanol-modified mobile phase on the separation of isotopically substituted compounds by micellar electrokinetic capillary chromatography, J. Microcol. Sep. 1 (1989) 125-130. doi:10.1002/mcs.1220010304.

[29] Y. Shao, L.F. Molnar, Y. Jung, J. Kussmann, C. Ochsenfeld, S.T. Brown, A.T. Gilbert, L.V. Slipchenko, S.V. Levchenko, D.P. O'Neill, R.A.Jr DiStasio, R.C. Lochan, T. Wang, G.J. Beran, N.A. Besley, J.M. Herbert, C.Y. Lin, T. Van Voorhis, S.H. Chien, A. Sodt, R.P. Steele, V.A. Rassolov, P.E. Maslen, P.P. Korambath, R.D. Adamson, B. Austin, J. Baker, E.F. Byrd, H. Dachsel, R.J. Doerksen, A. Dreuw, B.D. Dunietz, A.D. Dutoi, T.R. Furlani, S.R. Gwaltney, A. Heyden, S. Hirata, C.P. Hsu, G. Kedziora, R.Z. Khalliulin, P. Klunzinger, A.M. Lee, M.S. Lee, W. Liang, I. Lotan, N. Nair, B. Peters, E.I. Proynov, P.A. Pieniazek, Y.M. Rhee, J. Ritchie, E. Rosta, C.D. Sherrill, A.C. Simmonett, J.E. Subotnik, H.L.3rd Woodcock, W. Zhang, A.T. Bell, A.K. Chakraborty, D.M. Chipman, F.J. Keil, A. Warshel, W.J. Hehre, H.F. 3rd Schaefer, J. Kong, A.I. Krylov, P.M. Gill, M. Head-Gordon, Advances in methods and algorithms in a modern quantum chemistry program package, Phys. Chem. Chem. Phys. 8 (2006) 3172-3191. doi: 10.1039/B517914A.

[30] Gaussian 16, Revision C.01, M.J. Frisch, G.W. Trucks, H.B. Schlegel, G.E. Scuseria, M.A. Robb, J.R. Cheeseman, G. Scalmani, V. Barone, G.A. Petersson, H. Nakatsuji, X. Li, M. Caricato, A.V. Marenich, J. Bloino, B.G. Janesko, R. Gomperts, B. Mennucci, H.P. Hratchian, J.V. Ortiz, A.F. Izmaylov, J.L. Sonnenberg, D. Williams-Young, F. Ding, F. Lipparini, F. Egidi, J. Goings, B. Peng, A. Petrone, T. Henderson, D. Ranasinghe, V.G. Zakrzewski, J. Gao, N. Rega, G. Zheng, W. Liang, M. Hada, M. Ehara, K. Toyota, R. Fukuda, J. Hasegawa, M. Ishida, T. Nakajima, Y. Honda, O. Kitao, H. Nakai, T. Vreven, K. Throssell, J.A. Montgomery Jr., J.E. Peralta, F. Ogliaro, M.J. Bearpark, J.J. Heyd, E.N. Brothers, K.N. Kudin, V.N. Staroverov, T.A. Keith, R. Kobayashi, J. Normand, K. Raghavachari, A.P. Rendell, J.C. Burant, S.S. Iyengar, J. Tomasi, M. Cossi, J.M. Millam, M. Klene, C. Adamo, R. Cammi, J.W. Ochterski, R.L. Martin, K. Morokuma, O. Farkas, J.B. Foresman, D.J. Fox, Gaussian, Inc., Wallingford CT, (2016).

[31] S. Grimme, J. Antony, S. Ehrlich, H. Krieg, A consistent and accurate ab initio parameterization of density functional dispersion correction (DFT-D) for the 94 elements H-Pu, J. Chem. Phys. 132 (2010) 154104. doi: 10.1063/1.3382344.

[32] A.V. Marenich, C.J. Cramer, D.G. Truhlar, Universal solvation model based on solute electron density and a continuum model of the solvent defined by the bulk dielectric

589 constant and atomic surface tensions, J. Phys Chem. B. 113 (2009) 6378-6396. doi:
590 10.1021/jp810292n]

591 [33] T. Lu, F. Chen, Multiwfn: a multifunctional wavefunction analyser, J. Comput. Chem.
592 33 (2012) 580-592. doi: 10.1002/jcc.22885.

593 [34] T. Lu, F. Chen, Quantitative analysis of molecular surface based on improved
594 Marching Tetrahedra algorithm, J. Mol. Graph. Model. 38 (2012) 314-323. doi:
595 10.1016/j.jmgm.2012.07.004.

596 [35] S. Grimme, S. Ehrlich, L. Goerigk, Effect of the damping function in dispersion
597 corrected density functional theory, J. Comp. Chem. 32 (2011) 1456-1465. doi:
598 10.1002/jcc.21759.

599 [36] B. Chankvetadze, C. Yamamoto, Y. Okamoto, Enantioseparation of selected chiral
600 sulfoxides using polysaccharide-type chiral stationary phases and polar organic, polar
601 aqueous-organic and normal-phase eluents, J. Chromatogr. A 922 (2001) 127-137.
602 doi:10.1016/s0021-9673(01)00958-x.

603 [37] G. Jibuti, A. Mskhiladze, N. Takaishvili, M. Karchkhadze, L. Chankvetadze, T. Farkas,
604 B. Chankvetadze, HPLC separation of dihydropyridine derivatives enantiomers with
605 emphasis on elution order using polysaccharide-based chiral columns, J. Sep. Sci. 35
606 (2012) 2529-2537. doi:10.1002/jssc.201200443.

607 [38] I. Matarashvili, D. Ghughunishvili, L. Chankvetadze, N. Takaishvili, T. Khatiashvili,
608 M. Tsintsadze, T. Farkas, B. Chankvetadze, Separation of enantiomers of chiral weak
609 acids with polysaccharide-based chiral columns and aqueous-organic mobile phases in
610 high-performance liquid chromatography: Typical reversed-phase behavior? J.
611 Chromatogr. A. 1483 (2017) 86-92. doi:10.1016/j.chroma.2016.12.064.

612 [39] S. Materazzo, S. Carradori, R. Ferretti, B. Gallinella, D. Secci, R. Cirilli, Effect of the
613 water content on the retention and enantioselectivity of albendazole and fenbendazole
614 sulfoxides using amylose-based chiral stationary phases in organic-aqueous
615 conditions, J. Chromatogr. A. 1327 (2014) 73-79. doi:10.1016/j.chroma.2013.12.051.

616 [40] K. Kimata, K. Hosoya, T. Araki, N. Tanaka, Direct chromatographic separation of
617 racemates on the basis of isotopic chirality, Anal. Chem. 69 (1997) 2610-2612.
618 doi:10.1021/ac970338k.

619 [41] S. Puricelli, G. Bruno, C. Gatti, A. Ponti, M. Mella, Viability of hydrogen isotopes
620 separation via heterolytic dissociation-driven Chemical Affinity Quantum Sieving on
621 inexpensive alkali-earth oxides, Appl. Surf. Chem. 657 (2024) 159596.
622 https://doi.org/10.1016/j.apsusc.2024.159596.

623 [42] Y.Y. Zhan, Q.C. Jiang, K. Ishii, T. Koide, O. Kobayashi, T. Kojima, S. Takahashi, M.
624 Tachikawa, S. Uchiyama, S. Hiraoka, Polarizability and isotope effects on dispersion
625 interactions in water, Commun. Chem. 2 (2019) 141. doi: 10.1038/s42004-019-0242-
626 0.

627 [43] C. Zhao, R.M. Parrish, M.D. Smith, P.J. Pellechia, C.D. Sherrill, K.D. Shimizu, Do
628 deuteriums form stronger CH-π interactions? J. Am. Chem. Soc. 134 (2012) 14306-
629 14309. doi: 10.1021/ja305788p.

[44] T. Haino, K. Fukuta, H. Iwamoto, S. Iwata, Noncovalent isotope effect for guest encapsulation in self-assembled molecular capsules, Chem. Eur. J. 15 (2009) 13286-13290. doi: 10.1002/chem.200902526.

[45] E. Arunan, G.R. Desiraju, R.A. Klein, J. Sadlej, S. Scheiner, I. Alkorta, D.C. Clary, R.H. Crabtree, J.J. Dannenberg, P. Hobza, H.G. Kjaergaard, A.C. Legon, B. Mennucci, D.J. Nesbitt, Defining the hydrogen bond: An account (IUPAC Technical Report), Pure Appl. Chem. 83 (2011) 1619-1636. doi: 10.1351/PAC-REP-10-01-01.

Legends:

Fig. 1 Structure of AMP and MET isotopologues part of this study.

Fig. 2 Separation of AMP and AMP-d_5 on a Lux AMP (250 x 4.6 mm) column with the mobile phases made of MeOH with 0.1 % (v/v) ammonium hydroxide (a), 5 mM ammonium bicarbonate in H_2O (pH-11.0) and MeOH in the ratio (v/v) 10 : 90 (b) and 40 : 60 (c). Flow rate: 1 ml/min. MS-detection conditions were as described in Table 1.

Fig. 3 Separations of MET and MET-d_5 on a Lux AMP (250 x 4.6 mm) column with the mobile phases made of MeOH with 0.1% (v/v) ammonium hydroxide (a), 5 mM ammonium bicarbonate in H2O (pH-11.0) and MeOH in the ratio (v/v) 10 : 90 (b) and 40 : 60 (c). Flow rate: 1 ml/min. MS-detection conditions were as described in Table 1.

Fig. 4 Separation of AMP and AMP-d_5 on a Lux i-Amylose-3 (250 x 4.6 mm) column with the mobile phases made of MeOH with 0.1 % (v/v) ammonium hydroxide (a), 5 mM ammonium bicarbonate in H2O (pH-11.0) and MeOH in the ratio (v/v) 5 : 95 (b) and 50 : 50 (c). Flow rate: 1 ml/min. MS-detection conditions were as described in Table 1.

Fig. 5 Separation of AMP, AMP-d_5 (a), MET and MET-d_5 (b) on a Biphenyl (100 x 2.1mm) column with the mobile phase acetonitrile + 0.1% NH_4OH. Flow rate: 0.4 ml/min (a). MS-detection conditions were as described in Table 1.

Fig. 6 Separation of AMP, AMP-d_5 (a), MET and MET-d_5 (b) on a Lux i-Amylose-3 (250 x 4.6 mm) column with the mobile phase acetonitrile + 0.1% NH_4OH. Flow rate: 0.4 ml/min (a). MS-detection conditions were as described in Table 1.

Fig. 7 Separation of AMP and its isotopologues with various degree of deuteration on a Lux AMP (250 x 4.6 mm) column in the mobile phase: 5mM ammonium bicarbonate in H_2O (pH-11.0)/MeOH 40:60, Flow rate: 1ml/min. MS-detection conditions were as described in Table 1.

Fig. 8 DFT optimized structures for complexes between MET conformer **b** and benzene (A), 1,3-dimethylbenzene (B) and 1-chloro-3-methylbenzene (C). Legend colour: C, grey; Cl, green; H, pale grey; N, blue.

Fig. 9 Representative correlation between retention times of AMP isotopologues on the achiral Biphenyl column [MeOH/water 90:10 (A) and 20:80 (B)], quantum mechanics calculated vibrational frequencies (ν, cm^{-1}), and zero-point vibrational energy (ZPVE, Hartree/particle): AMP conformer **a**; SMD, MeOH (A), AMP_conformer **b**; SMD, water (B).

Fig. 10 Representative correlation between retention times of AMP isotopologues on the achiral Biphenyl column (MeOH/water 70:30), quantum mechanics calculated vibrational frequencies (ν, cm^{-1}) and zero-point vibrational energy (ZPVE, Hartree/particle): AMP_conformer **a**; SMD, MeOH.

Figure 1

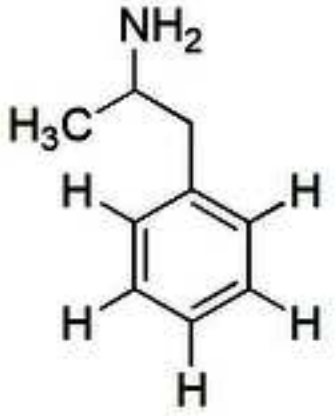

AMP

AMP-$d_{5(side\ chain)}$

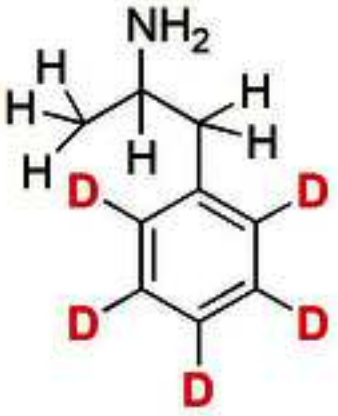

AMP-$d_{5(ring)}$

AMP-d_6

AMP-d_8

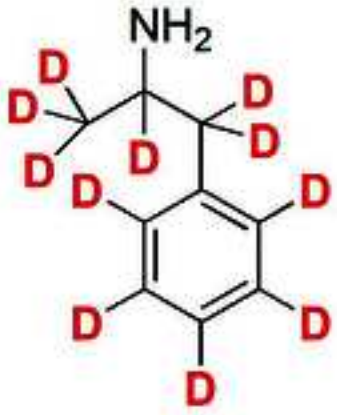

AMP-d_{11}

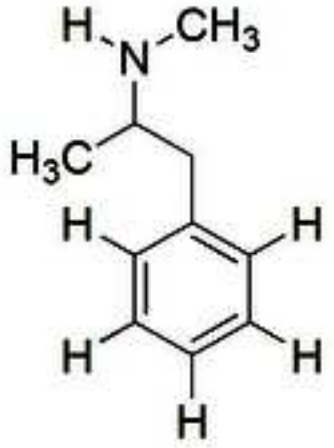

MET

MET-d_5

Figure 2

Click here to access/download;Figure;Folie2.TIF

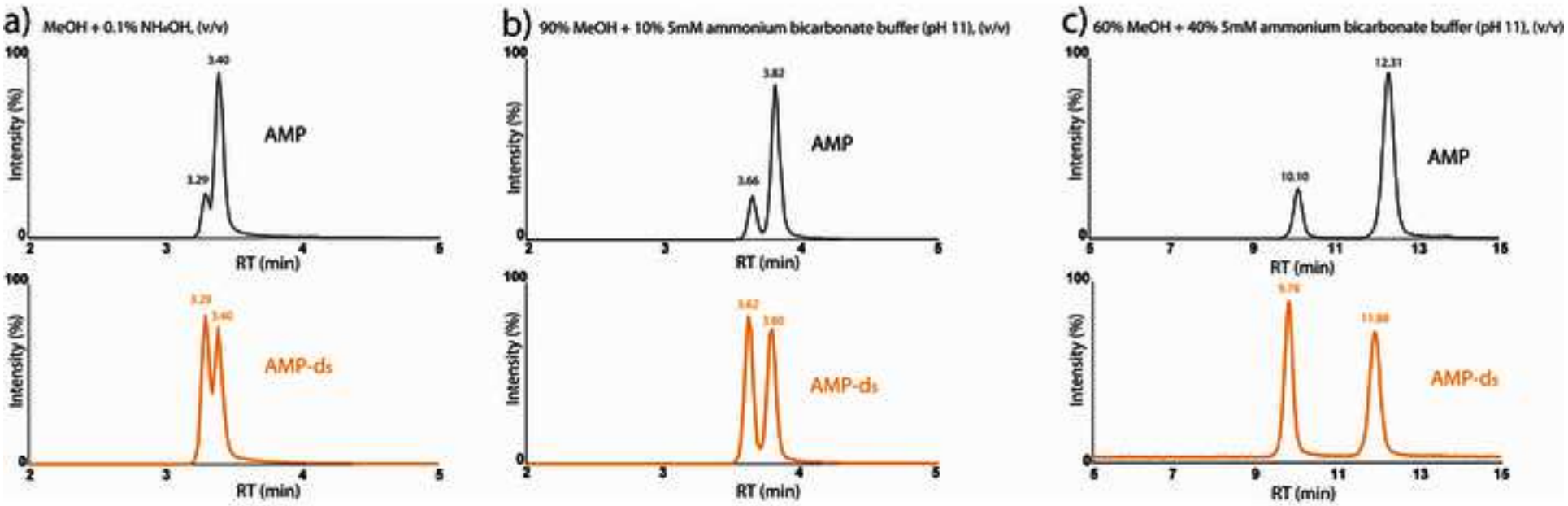

Fig. 2

Figure 3

Click here to access/download;Figure;Folie3.TIF

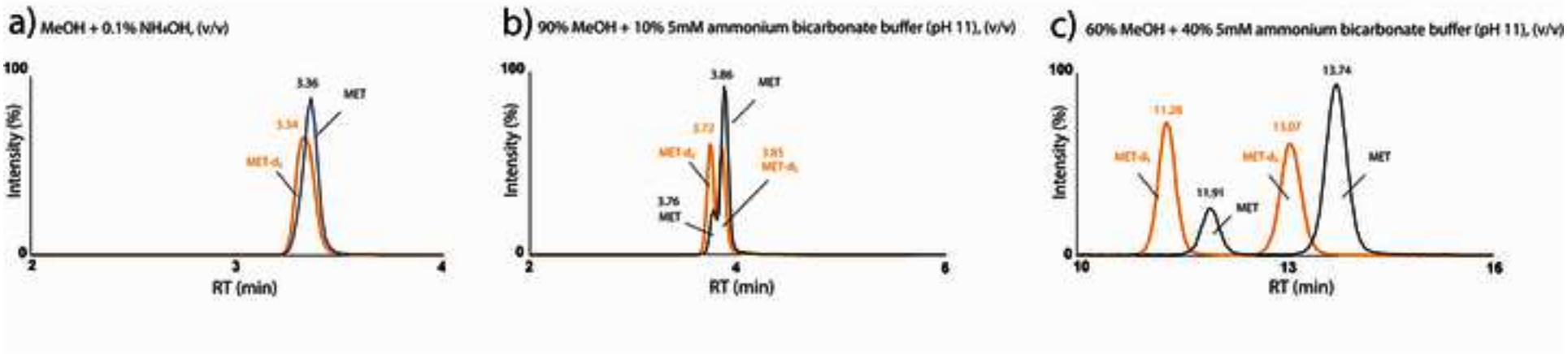

Fig. 3

Figure 4

Click here to access/download;Figure;Folie4.TIF

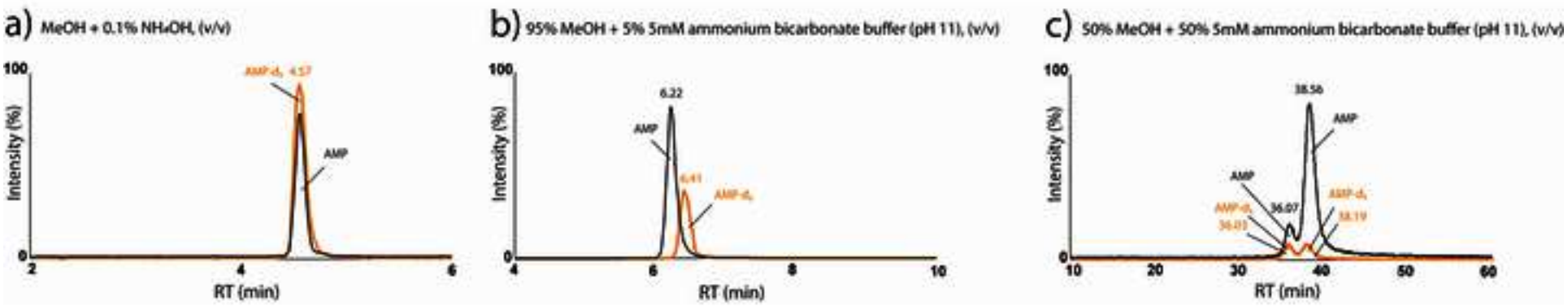

Fig. 4

Figure 5

Click here to access/download;Figure;Folie5.TIF

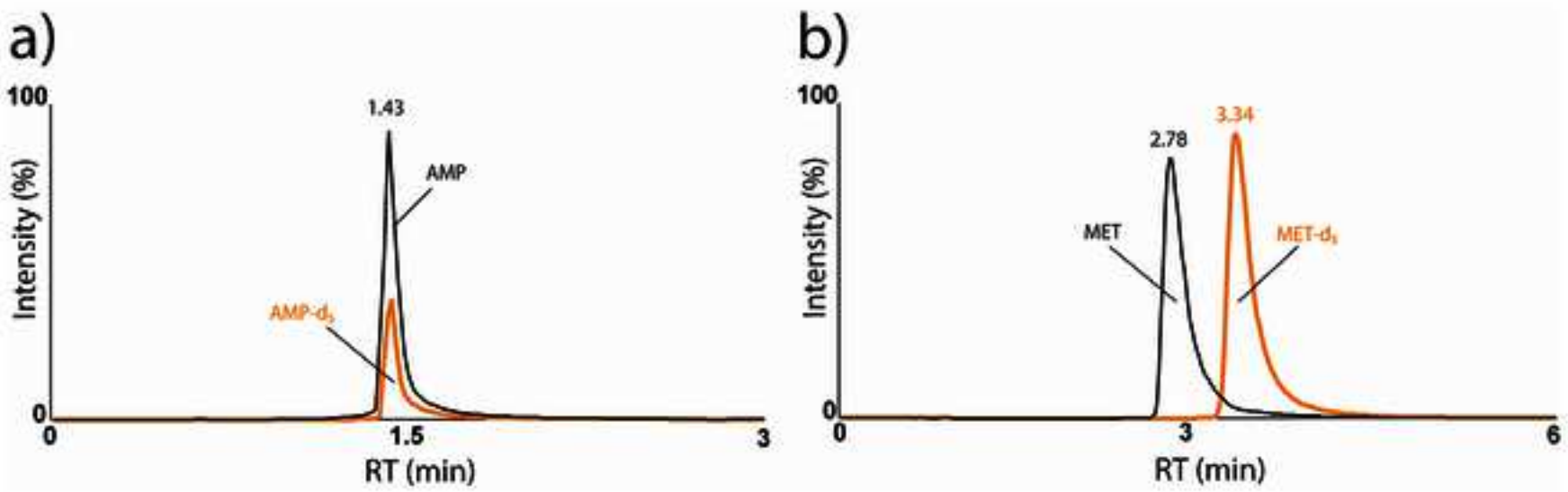

Fig. 5

Figure 6

Click here to access/download;Figure;Folie6.TIF

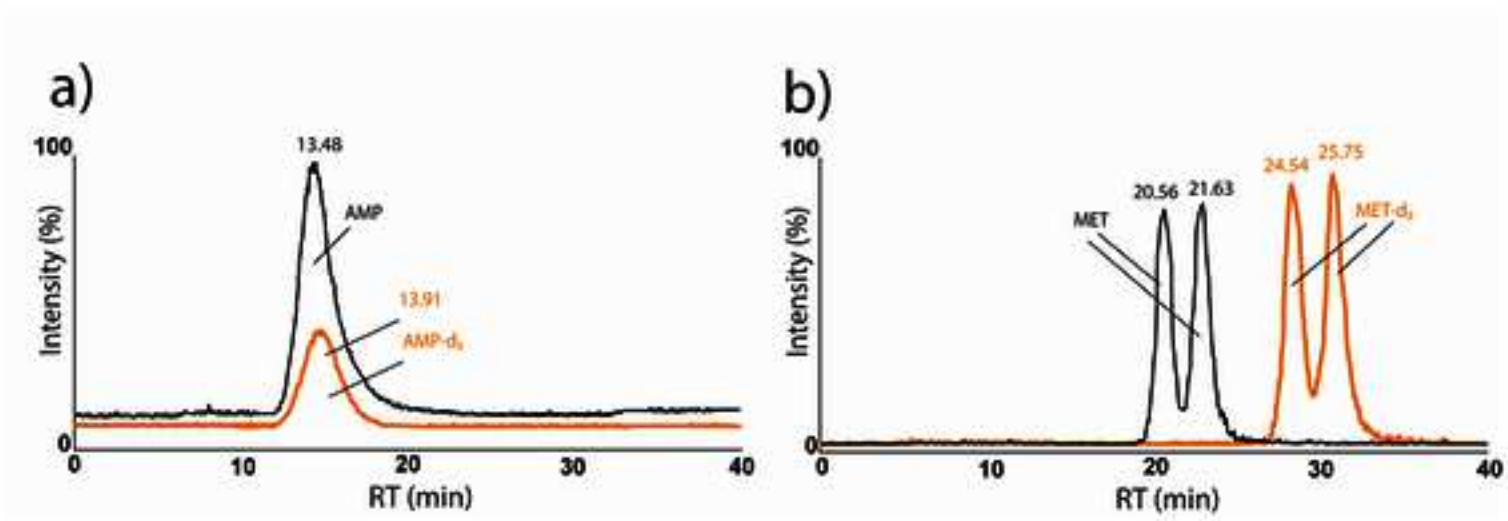

Fig. 6

Figure 7

Click here to access/download;Figure;Folie7.TIF

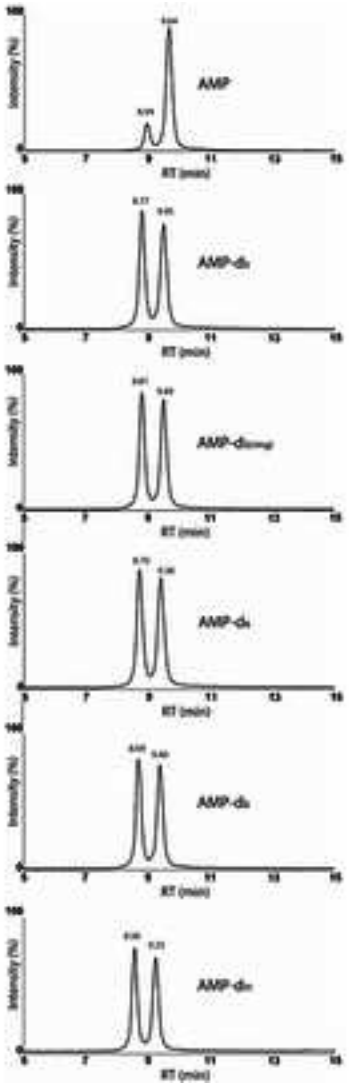

Fig. 7

Figure 8

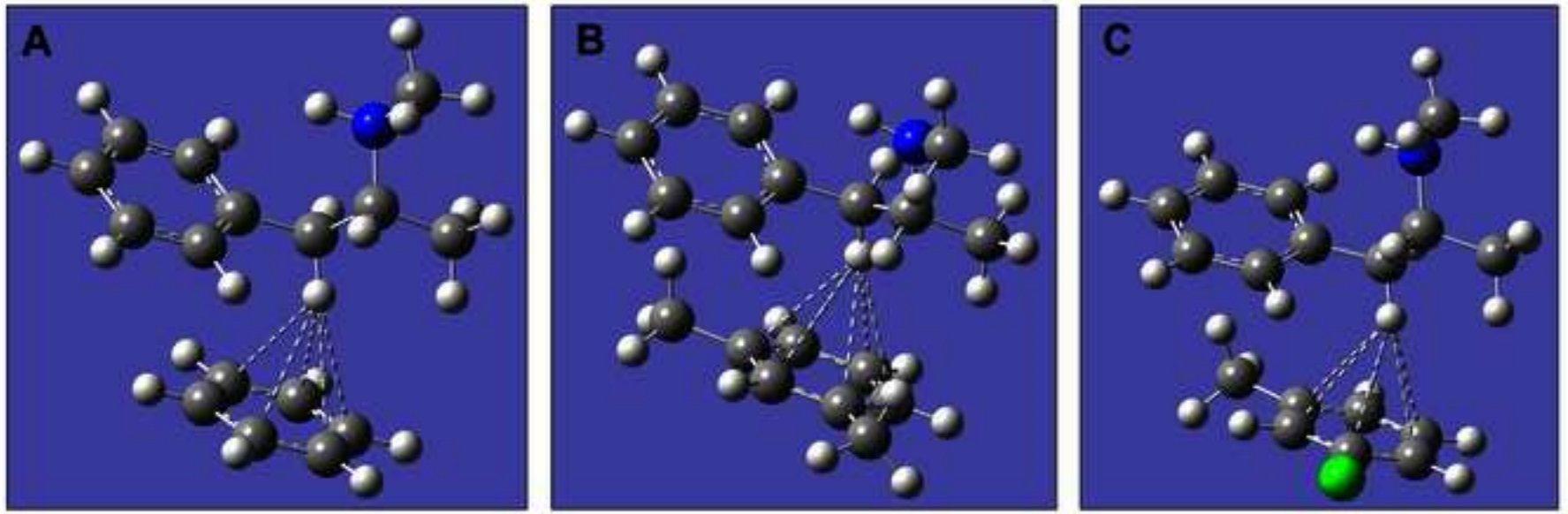

Figure 9

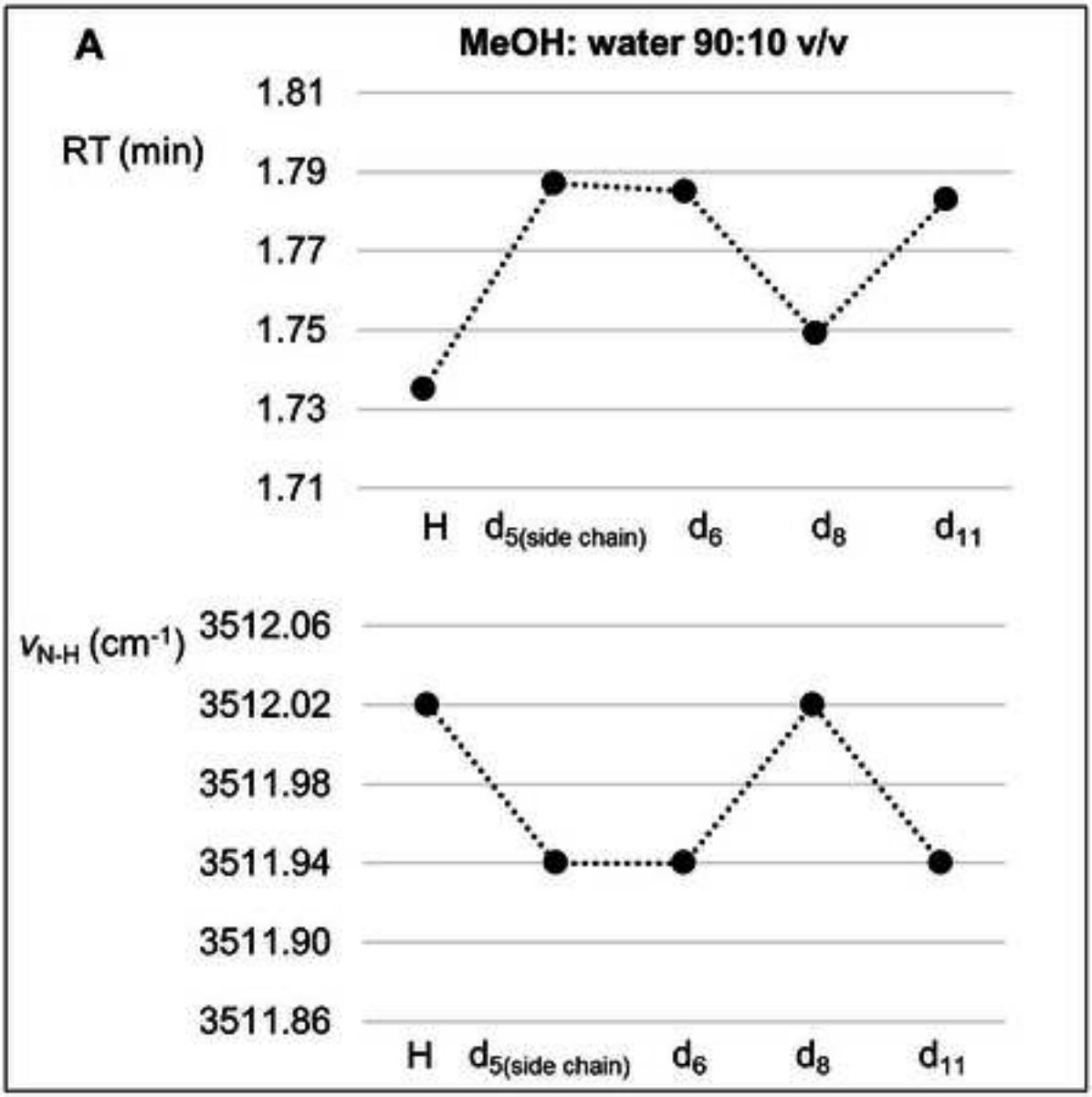

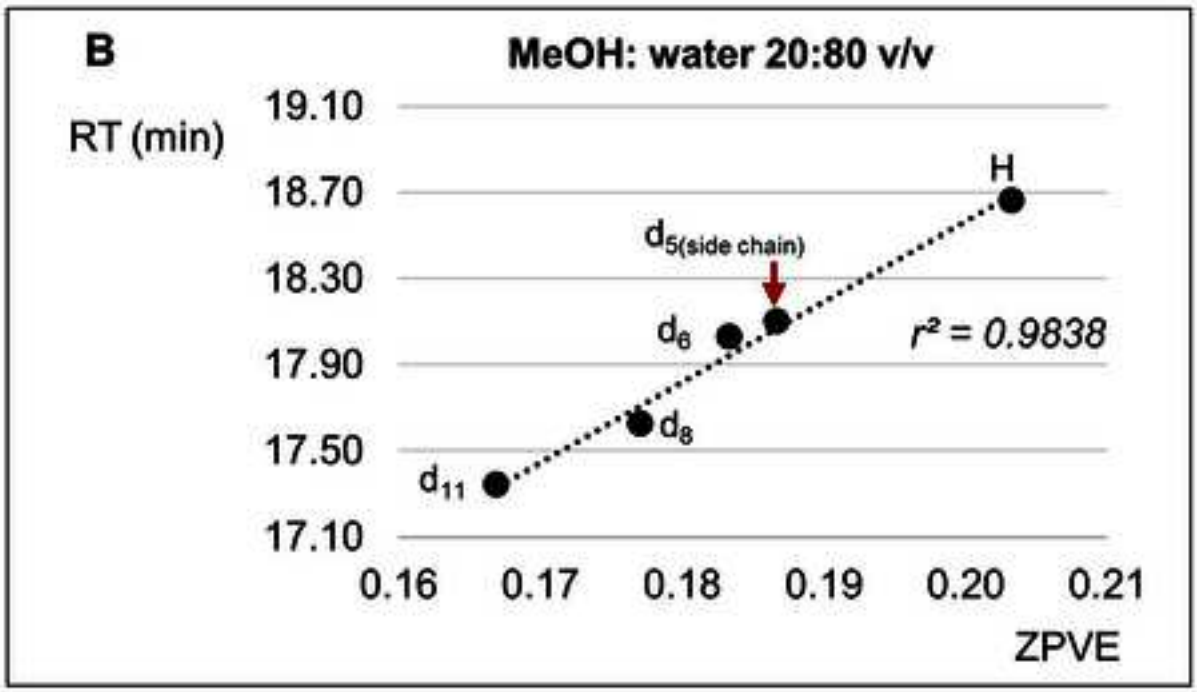

Figure 10

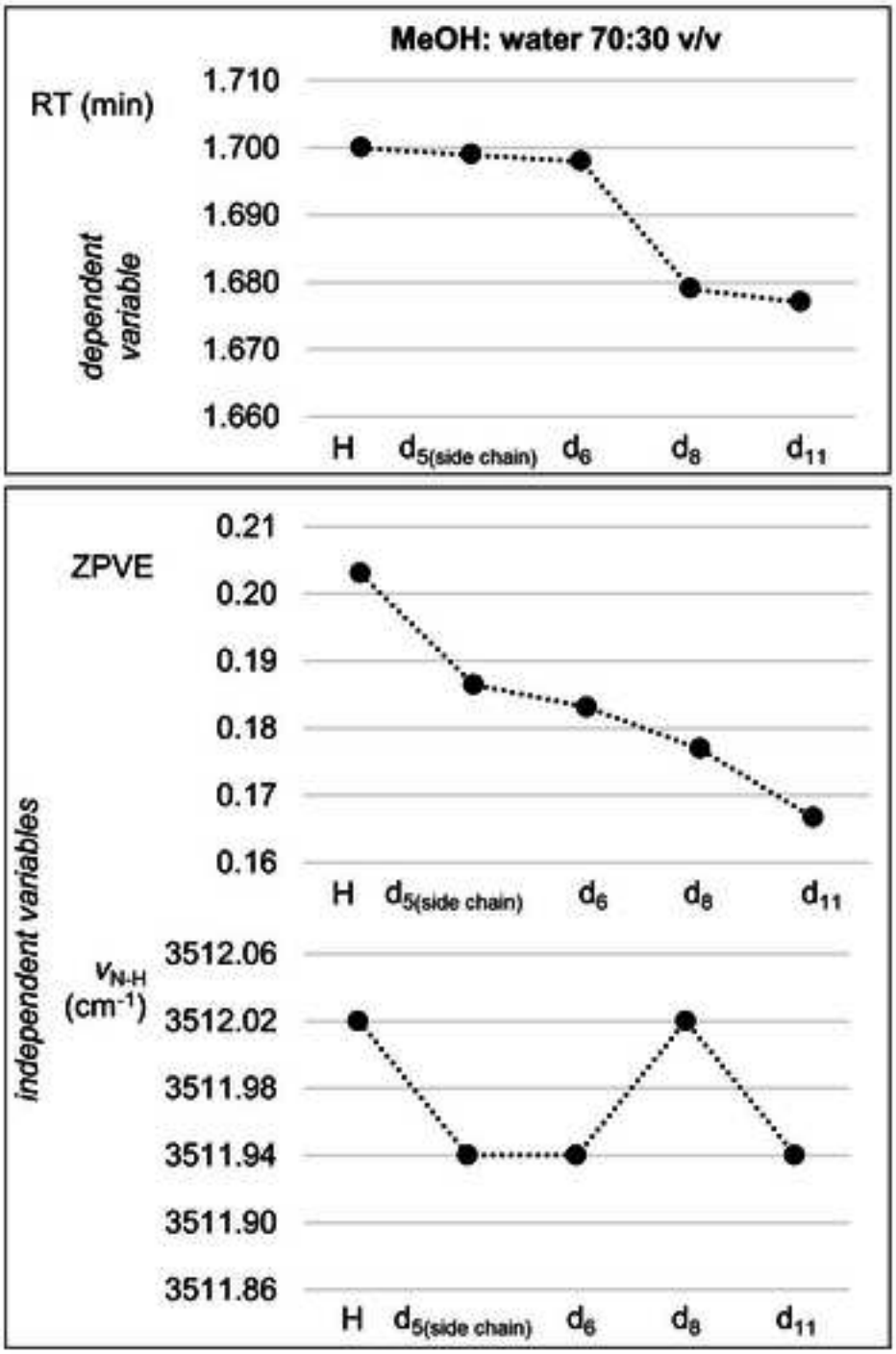

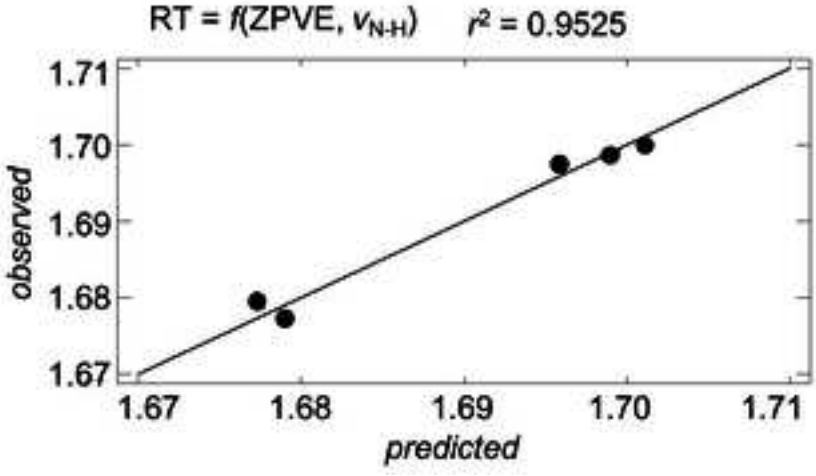

Table 1 Mass spectrometry parameters for analytes and internal standards in the positive ionization mode.

Analytes	Molecular mass, g/mol	Precursor ion, m/z	Product ion, m/z	CE, eV
AMPHETAMINE	135.1	136.1	119.1	5
			91.1	13
AMPHETAMINE-$d_{5(\text{side chain})}$	140.2	141.25	124.1	8
			93.1	24
AMPHETAMINE-$d_{5(\text{ring})}$	140.2	141.25	96.1	16
			68.1	44
AMPHETAMINE-d_6	141.2	142.25	125.1	8
			93.1	16
AMPHETAMINE-d_8	143.2	144.25	127.1	8
			97.1	16
AMPHETAMINE-d_{11}	146.28	147.28	130.1	8
			98.1	24
METHAMPHETAMINE	149.2	150.2	119.1	8
			91.1	20
METHAMPHETAMINE-d_5	154.1	155.1	121.1	8
			92.1	20

Electronic Supplementary Material (online publication only)

Click here to view linked References

Declaration of Interest Statement

The authors declare that they have no known competing financial interests or personal relationships that could have appeared to influence the work reported in this paper.